International Journal of Solids and Structures 91 (2016) 18–25

Contents lists available at ScienceDirect

International Journal of Solids and Structures

journal homepage: www.elsevier.com/locate/ijsolstr

Manipulating pressure and shear waves in dielectric elastomers via external electric stimuli

Pavel I. Galich, Stephan Rudykh*

Department of Aerospace Engineering, Technion – Israel Institute of Technology, Haifa 32000, Israel

ARTICLE INFO

Article history:
Received 31 December 2015
Revised 19 April 2016
Available online 3 May 2016

Keywords:
Elastic waves
Non-linear electroelasticity
Dielectric elastomers
Finite deformation

ABSTRACT

We investigate elastic wave propagation in finitely deformed dielectric elastomers in the presence of an electrostatic field. To analyze the propagation of both longitudinal (P-) and transverse (S-) waves, we utilize *compressible* material models. We derive explicit expressions for the generalized acoustic tensor and phase velocities of elastic waves for ideal and enriched dielectric elastomer models. We analyze the slowness curves of elastic wave propagation, and find the P-S-mode disentangling phenomenon. In particular, P-and S-waves can be separated by applying an electric field. The divergence angle between P-and S-waves strongly depends on the applied electrostatic excitation. The influence of an electric field depends on the choice of a material model. In the case of the ideal dielectric model, the in-plane shear wave velocity increases with an increase in electric field, while for the enriched model the velocity may decrease depending on material constants. The divergence angle also gradually increases with an increase in electric field, while for the enriched model the angle variation may be limited. Material compressibility affects the P-wave velocity, and for relatively compressible materials the slowness curve of the P-wave evolves from circular to elliptical shape manifesting in an increase in the refraction angle of the P-wave. As a result, the divergence angle decreases with an increase in material compressibility.

1. Introduction

Dielectric elastomers (DEs) are soft responsive materials that can change their form and shape when subjected to an electric stimulus (Pelrine et al., 2000; Bar-Cohen, 2002). DEs have attracted considerable attention due to a large variety of possible applications ranging from artificial muscles and soft robotics to energy conversion and noise canceling devices (O'Halloran et al., 2008; Brochu and Pei, 2010; Carpi et al., 2011; Rudykh et al., 2012; Kornbluh et al., 2012; Rogers, 2013). The theoretical framework of the non-linear electroelasticity is based on a theory first developed by Toupin (1956; 1963), which was recently revisited by Dorfmann and Ogden (2005; 2010) and Suo et al. (2008); Suo (2010). This followed by a series of works on modeling DEs (Volokh, 2012; Itskov and Khiêm, 2014; Keip et al., 2014; Cohen and deBotton, 2014; Jabareen, 2015; Miehe et al., 2015; Aboudi, 2015; Hossain et al., 2015; Cohen et al., 2016), to name a few recent contributions. The electromechanical coupling in typical DEs is rather weak, and, therefore, DEs need to operate at the edge of instabilities and breakthrough voltages to achieve meaningful actuation (Zhao et al., 2007; Zhao and Suo, 2008; 2010; Rudykh and deBotton, 2011; Rudykh et al., 2014; Rudykh and Bertoldi, 2013; Gei et al., 2014; Siboni et al., 2014; Bortot et al., 2016). Potentially, the need for the high voltage can be reduced through architectured microstructures of DEs increasing the electromechanical coupling (Huang et al., 2004; Rudykh et al., 2013; Cao and Zhao, 2013; Galipeau et al., 2014; Chatzigeorgiou et al., 2015). Moreover, synthesis of new soft dielectric materials seems to be another promising approach (Madsen et al., 2014). The effective electromechanical properties of DEs can be actively controlled by external electric stimuli. The dominant factor is the finite deformations induced by an electric excitation. Since in purely elastic materials wave propagation strongly depends on the mechanical properties of the media and deformation fields (Rudykh and Boyce, 2014; Galich and Rudykh, 2015b; 2015a), this opens an opportunity to manipulate wave propagation in DEs by applying an electric field.

In this work, we focus on elastic wave propagation in finitely deformed DEs in the presence of a uniform electric field. To explore the elastic wave propagation in DEs, we follow the widely used approach for the analysis of small-amplitude motions superimposed on the finite deformations (Ogden, 1997) induced by an external stimulus (Dorfmann and Ogden, 2010; Destrade and Ogden, 2011). To allow for the consideration of the longitudinal wave propagation (differently from the recent works (Gei et al., 2011; Shmuel et al., 2012; Chen and Dai, 2012), where incompressible

* Corresponding author. Tel.: +972 48292547.
E-mail address: rudykh@technion.ac.il (S. Rudykh).

http://dx.doi.org/10.1016/j.ijsolstr.2016.04.032
0020-7683/

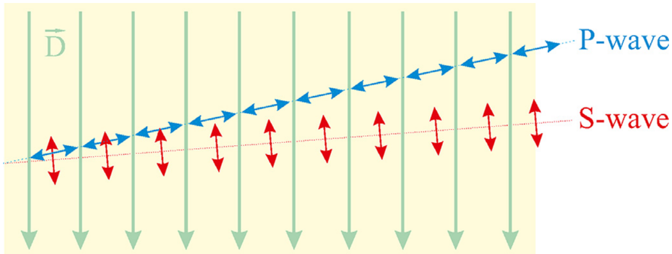

Fig. 1. Schematics of the splitting of pressure (P-) and shear (S-) elastic waves in a nearly incompressible neo-Hookean DE. P-wave does not refract from the initial direction of propagation, while S-wave refracts at a certain angle.

materials were considered), we utilize *compressible* electroactive material models, namely the ideal (Zhao et al., 2007) and enriched DE models. By application of wave propagation analysis to the compressible DE models, we derive explicit expressions for the generalized acoustic tensor and phase velocities for both longitudinal and transverse waves. We find that electrostatically induced changes in the key characteristics of shear (S-) and pressure (P-) waves lead to a disentangling phenomenon, where P-and S-waves travel in different directions. Fig. 1 schematically illustrates the P-and S-wave splitting phenomenon. The divergence angle strongly depends on the external field, the induced deformation, and material compressibility. P-and S-waves possess diverse properties and, thus, can be used for different purposes. For example, the S-wave serves as a virtual "finger" to probe elasticity of internal regions of the body in shear wave elasticity imaging (Sarvazyan et al., 1998). Longitudinal and transversal elastic waves can be separated at the interface between dissimilar materials; however, this may cause a loss of energy or/and a wave-mode conversion at the interface (Achenbach, 1973). Alternatively, we can use dielectric elastomers to split P-and S-elastic waves by applying a bias electric field. This feature can be employed, for example, in small-scale micro-electromechanical systems, where it is convenient to use an electric field to control the performance. Moreover, due to mathematical similarities between electro- and magneto-active materials, this splitting phenomenon can be utilized in magnetorheological elastomers controlled by an external magnetic field.

2. Analysis

To analyze the finitely deformed state, we introduce the deformation gradient $\mathbf{F}(\vec{X},t) = \nabla_{\vec{X}} \otimes \vec{x}(\vec{X},t)$, where $\vec{X}$ and $\vec{x}$ are position vectors in the reference and current configurations, respectively. In order to model a non-linear electroelastic material behavior, we consider an energy function $\psi(\mathbf{F},\vec{D}_0)$, which is a function of deformation gradient $\mathbf{F}$ and electric displacement vector $\vec{D}_0$ in the reference configuration. The corresponding electric displacement in the current configuration is given by $\vec{D} = J^{-1}\mathbf{F}\cdot\vec{D}_0$, where $J \equiv \det \mathbf{F} > 0$. The first Piola–Kirchhoff stress tensor and electric field in the reference configuration are given by

$$\mathbf{P}_0 = \frac{\partial \psi}{\partial \mathbf{F}} \quad \text{and} \quad \vec{E}_0 = \frac{\partial \psi}{\partial \vec{D}_0}, \tag{1}$$

the corresponding counterparts in the current configuration are

$$\mathbf{T} = J^{-1}\mathbf{P}_0\cdot\mathbf{F}^T \quad \text{and} \quad \vec{E} = \mathbf{F}^{-T}\cdot\vec{E}_0. \tag{2}$$

Linearized constitutive Eqs. (1) read as

$$\delta\mathbf{P}_0 = \mathbb{C}_0 : \delta\mathbf{F} + \mathcal{M}_0\cdot\delta\vec{D}_0 \quad \text{and} \quad \delta\vec{E}_0 = \delta\mathbf{F} : \mathcal{M}_0 + \mathbf{K}_0\cdot\delta\vec{D}_0, \tag{3}$$

where δ denotes an incremental change; $\mathbb{C}_0, \mathcal{M}_0$ and $\mathbf{K}_0$ are the so-called tensors of electroelastic moduli (Dorfmann and Ogden, 2010) defined as

$$\mathbb{C}_0 = \frac{\partial^2\psi}{\partial\mathbf{F}\partial\mathbf{F}}, \quad \mathcal{M}_0 = \frac{\partial^2\psi}{\partial\mathbf{F}\partial\vec{D}_0} \quad \text{and} \quad \mathbf{K}_0 = \frac{\partial^2\psi}{\partial\vec{D}_0\partial\vec{D}_0}. \tag{4}$$

Note that $\mathbb{C}_0 = \mathbb{C}_0^{(3412)}$ and $\mathbf{K}_0 = \mathbf{K}_0^T$; here the superscript (3412) denotes an isomer of the fourth-rank tensor (Galich and Rudykh, 2015b; Ryzhak, 1993; Nikitin and Ryzhak, 2008) as detailed in Appendix A.

Next, we consider the small-amplitude motions superimposed on finite deformations; hence, we present the incremental constitutive Eqs. (3) in the frame of the updated reference configuration

$$\delta\mathbf{P} = \mathbb{C} : \delta\mathbf{H} + \mathcal{M}\cdot\delta\vec{D}_{01} \quad \text{and} \quad \delta\vec{E}_{01} = \delta\mathbf{H} : \mathcal{M} + \mathbf{K}\cdot\delta\vec{D}_{01}, \tag{5}$$

where $\delta\mathbf{P} = J^{-1}\delta\mathbf{P}_0\cdot\mathbf{F}^T$, $\delta\vec{D}_{01} = J^{-1}\mathbf{F}\cdot\delta\vec{D}_0$, $\delta\vec{E}_{01} = \mathbf{F}^{-T}\cdot\delta\vec{E}_0$, $\delta\mathbf{H} = \delta\mathbf{F}\cdot\mathbf{F}^{-1}$,

$$\mathbb{C} = J^{-1}\left(\mathbf{F}\cdot\mathbb{C}_0^{(2134)}\cdot\mathbf{F}^T\right)^{(2134)}, \quad \mathcal{M} = \mathbf{F}\cdot\mathcal{M}_0^{(213)}\cdot\mathbf{F}^{-1} \text{ and } \mathbf{K} = J\mathbf{F}^{-T}\cdot\mathbf{K}_0\cdot\mathbf{F}^{-1}. \tag{6}$$

Note that $\mathbb{C} = \mathbb{C}^{(3412)}$, $\mathcal{M}^{(213)} = \mathcal{M}$ and $\mathbf{K} = \mathbf{K}^T$. The linearized equation of motion and Maxwell's equations in Eulerian form are

$$\nabla_{\vec{x}}\cdot\delta\mathbf{P} = \rho\frac{\partial^2\vec{u}}{\partial t^2}, \quad \nabla_{\vec{x}}\times\delta\vec{E}_{01} = 0 \quad \text{and} \quad \nabla_{\vec{x}}\cdot\delta\vec{D}_{01} = 0, \tag{7}$$

where $\vec{u}$ is the incremental displacement; $\rho = \rho_0/J$ is the density of the deformed material and ρ_0 is the initial density of the material. We assume the absence of free body charges and currents. Note that we use the so called quasi-electrostatic approximation (Dorfmann and Ogden, 2010; Maugin, 1985); more specifically, the interactions between electric and magnetic fields are neglected. This is the non-relativistic approximation corresponding to the case where the mechanical velocity is significantly smaller than the light velocity (Dorfmann and Ogden, 2010).

We seek for a solution for Eqs. (7) in the form of plane waves with constant polarizations

$$\vec{u} = \vec{m}f(\vec{n}\cdot\vec{x} - ct) \quad \text{and} \quad \delta\vec{D}_{01} = \vec{d}g(\vec{n}\cdot\vec{x} - ct), \tag{8}$$

where f is a twice continuously differentiable function and g is a continuously differentiable function; unit vectors $\vec{m}$ and $\vec{d}$ are polarization vectors of mechanical and electrical displacements, respectively; the unit vector $\vec{n}$ defines the direction of wave propagation, and c is the phase velocity of the wave.

Substituting (5) and (8) into (7), we obtain

$$\mathbf{A}\cdot\vec{m} = \rho c^2\vec{m}, \tag{9}$$

where $\mathbf{A}$ is the so-called "generalized" acoustic tensor defining the condition of propagation of elastic plane waves in non-linear electroelastic materials. The generalized acoustic tensor of electroelastic materials with an arbitrary strain energy function $\psi(\mathbf{F},\vec{D}_0)$, has the following form (Destrade and Ogden, 2011; Spinelli and Lopez-Pamies, 2015)

$$\mathbf{A} = \mathbf{Q} - \frac{2}{(\mathrm{tr}\hat{\mathbf{K}})^2 - \mathrm{tr}\hat{\mathbf{K}}^2}\mathbf{R}\cdot\left((\mathrm{tr}\hat{\mathbf{K}})\hat{\mathbf{I}} - \hat{\mathbf{K}}\right)\cdot\mathbf{R}^T, \tag{10}$$

where

$$\hat{\mathbf{I}} = \mathbf{I} - \vec{n}\otimes\vec{n} \tag{11}$$

is the projection on the plane normal to $\vec{n}$, $\hat{\mathbf{K}} = \hat{\mathbf{I}}\cdot\mathbf{K}\cdot\hat{\mathbf{I}}$, and

$$\mathbf{Q} = \mathbb{C}^{(1324)} : \vec{n}\otimes\vec{n} \quad \text{and} \quad \mathbf{R} = \vec{n}\cdot\mathcal{M}. \tag{12}$$

Note that the generalized acoustic tensor $\mathbf{A}$ and the purely elastic acoustic tensor $\mathbf{Q}$ are symmetric. Recall that for DE to be stable, the generalized acoustic tensor $\mathbf{A}$ has to be positively defined. Note that an analogue of the generalized acoustic tensor (10) was derived by Destrade and Ogden (2011) for incompressible magnetoelastic materials.

A detailed description of the non-linear electroelastic theory for DEs can be found in publications of Dorfmann and Ogden (2005; 2010), and Suo et al. (2008), Suo (2010).

It is well known that incompressible materials do not support longitudinal waves. Therefore, to analyze both transversal and longitudinal waves, we consider the energy function $\psi(\mathbf{F}, \vec{D}_0)$ for the *compressible* electroelastic material in the following form:

$$\psi(\mathbf{F}, \vec{D}_0) = \psi_{elas}(\mathbf{F}) + \frac{1}{2\epsilon J}(\gamma_0 I_{4e} + \gamma_1 I_{5e} + \gamma_2 I_{6e}), \tag{13}$$

where $\psi_{elas}(\mathbf{F})$ is a purely elastic energy function (for example, neo-Hookean, Mooney–Rivlin, Gent, etc. (Ogden, 1997)), ϵ is the material permittivity in the undeformed state ($\mathbf{F} = \mathbf{I}$) and γ_i are dimensionless parameters, moreover $\gamma_0 + \gamma_1 + \gamma_2 = 1$, and

$$I_{4e} = \vec{D}_0 \cdot \vec{D}_0, \quad I_{5e} = \vec{D}_0 \cdot \mathbf{C} \cdot \vec{D}_0 \quad \text{and} \quad I_{6e} = \vec{D}_0 \cdot \mathbf{C}^2 \cdot \vec{D}_0 \tag{14}$$

are invariants depending on the electric displacement $\vec{D}_0$ and right Cauchy-Green tensor $\mathbf{C} = \mathbf{F}^T \cdot \mathbf{F}$.

For the energy function (13) the relation between the electric field and displacement is

$$\vec{E} = \frac{1}{\epsilon}\left(\gamma_0 \mathbf{B}^{-1} + \gamma_1 \mathbf{I} + \gamma_2 \mathbf{B}\right) \cdot \vec{D}, \tag{15}$$

where $\mathbf{B} = \mathbf{F} \cdot \mathbf{F}^T$ is the left Cauchy–Green tensor. The corresponding tensors of electroelastic moduli are

$$\mathbb{C} = \mathbb{C}_{elas} + \frac{1}{2\epsilon}\left(\gamma_0 \mathbb{C}_{4e} + \gamma_1 \mathbb{C}_{5e} + \gamma_2 \mathbb{C}_{6e}\right),$$
$$\mathcal{M} = \frac{1}{2\epsilon}\left(\gamma_0 \mathcal{M}_{4e} + \gamma_1 \mathcal{M}_{5e} + \gamma_2 \mathcal{M}_{6e}\right) \quad \text{and}$$
$$\mathbf{K} = \frac{1}{\epsilon}\left(\gamma_0 \mathbf{B}^{-1} + \gamma_1 \mathbf{I} + \gamma_2 \mathbf{B}\right), \tag{16}$$

where $\mathbb{C}_{elas}$ is derived from the purely elastic part $\psi_{elas}(\mathbf{F})$ of the energy function in accordance to (4) and (6); and the explicit expressions for the other tensors are given in Appendix B.

Finally, the corresponding generalized acoustic tensor takes the following form

$$\mathbf{A} = \mathbf{Q}_{elas} + \frac{1}{2\epsilon}\left(\gamma_0 \mathbf{Q}_{4e} + \gamma_1 \mathbf{Q}_{5e} + \gamma_2 \mathbf{Q}_{6e} - \frac{4}{\eta}\mathbf{A}_e\right), \tag{17}$$

where $\mathbf{Q}_{elas}$ is calculated by applying of Eqs. (4), (6) and (12) to the purely elastic part $\psi_{elas}(\mathbf{F})$ of the energy function; the explicit expressions for η, and tensors $\mathbf{Q}_{4e}$, $\mathbf{Q}_{5e}$, $\mathbf{Q}_{6e}$ and $\mathbf{A}_e$ are given in the Appendix B. Remarkably, in the particular case of $\mathbf{F} = \lambda_1 \vec{e}_1 \otimes \vec{e}_1 + \lambda_2 \vec{e}_2 \otimes \vec{e}_2 + \lambda_3 \vec{e}_3 \otimes \vec{e}_3$, $\vec{n} = \vec{e}_1$ and $\vec{D}_0 = D_2 \vec{e}_2$, the generalized acoustic tensor (17) reduces to

$$\mathbf{A} = \mathbf{Q}_{elas} + \frac{\gamma_2 D_2^2}{\epsilon \lambda_3^2} \vec{e}_2 \otimes \vec{e}_2, \tag{18}$$

here the set of $(\vec{e}_1, \vec{e}_2, \vec{e}_3)$ defines the orthonormal basis.

Let us consider the influence of an electric field on the P-and S-waves propagation. Important characteristics of elastic waves can be deduced from the consideration of slowness curves. Fig. 2 (a) schematically shows the slowness curves for P-and S-waves propagating in a DE subjected to an electric field. P-and S-waves refract differently from the initial direction of propagation, thus, the P-and S-waves can be split in such media. The normals to the slowness curves can be defined by the corresponding angle θ (see Fig. 2 (a))

$$\tan\theta_{p,s} = \frac{s_{p,s}\sin\varphi - (ds_{p,s}/d\varphi)\cos\varphi}{s_{p,s}\cos\varphi + (ds_{p,s}/d\varphi)\sin\varphi}, \tag{19}$$

where φ is the incident angle and $s_{p,s}(\varphi) = c_{p,s}^{-1}(\varphi)$ are slownesses of P-and S-waves, respectively. Consequently, the divergence angle between P-and S-wave can be calculated as $\Delta\theta = \theta_p - \theta_s$.

3. Results

3.1. Ideal dielectric elastomer model

First, we consider an ideal dielectric elastomer model (Zhao et al., 2007), namely $\gamma_0 = \gamma_2 = 0$ and $\gamma_1 = 1$ in (13). For the elastic part of the energy function (13), here and thereafter, we utilize a model of a compressible neo-Hookean material (Ogden, 1997)

$$\psi_{elas}(\mathbf{F}) = \frac{\mu}{2}(I_1 - 3) - \mu \ln J + \left(\frac{K}{2} - \frac{\mu}{3}\right)(J-1)^2, \tag{20}$$

where $I_1 = \mathrm{tr}\,\mathbf{C}$ is the first invariant of the right Cauchy-Green tensor, μ is the shear modulus and K is the bulk modulus.

For the ideal DE, the generalized acoustic tensor takes the form

$$\mathbf{A} = a_1^* \vec{n} \otimes \vec{n} + a_2^* \hat{\mathbf{I}}, \tag{21}$$

where $\vec{n} \otimes \vec{n}$ is the projection on the direction $\vec{n}$ and $\hat{\mathbf{I}}$ is given in (11),

$$a_1^* = (K - 2\mu/3)J + \mu J^{-1}(1 + \vec{n} \cdot \mathbf{B} \cdot \vec{n}) \tag{22}$$

and $\quad a_2^* = \mu J^{-1}(\vec{n} \cdot \mathbf{B} \cdot \vec{n}). \quad (23)$

Consequently, there always exist one pressure and two shear waves for any direction of propagation $\vec{n}$, finite deformation $\mathbf{F}$ and electric displacement $\vec{D}$. The phase velocities of these waves can be calculated as

$$c_p = \sqrt{a_1^* J/\rho_0} \quad \text{and} \quad c_s = \sqrt{a_2^* J/\rho_0}. \tag{24}$$

Remarkably, while the electroelastic moduli (16) explicitly depend on the electric field, the phase velocities of elastic waves do not explicitly depend on the electric field. The dependence of the velocities on an electric field is introduced through the electrostatically induced deformation. Let us consider the case when $\vec{D}_0 = D\sqrt{\mu\epsilon}\,\vec{e}_2$, DE can freely expand in plane $\vec{e}_1 - \vec{e}_3$, and the deformation gradient can be expressed as

$$\mathbf{F} = \lambda(D)\vec{e}_2 \otimes \vec{e}_2 + \tilde{\lambda}(D)(\mathbf{I} - \vec{e}_2 \otimes \vec{e}_2). \tag{25}$$

For an incompressible ideal DE (Zhao et al., 2007), the stretch ratios can be expressed as $\lambda = (1 + D^2)^{-1/3}$ and $\tilde{\lambda} = \lambda^{-1/2}$. It should be noted that these relations approximately hold even for very compressible materials with $K/\mu \sim 1$ for the range of deformations and electric fields considered here. Recall that neo-Hookean DE is stable for $D \leqslant \sqrt{3}$ (Zhao et al., 2007) and it will thin down without any limit when the electric field is further increased. Note that in the absence of an electric field, expressions (24) reduce to $c_p = \sqrt{(K + 4\mu/3)/\rho_0}$ and $c_s = \sqrt{\mu/\rho_0}$.

For the nearly incompressible DE, the phase velocities of P-and S-waves can be calculated as

$$c_p = \sqrt{\left((K + \mu/3 + \frac{\mu\left(1 + D^2\cos^2\varphi\right)}{\left(1 + D^2\right)^{2/3}}\right)/\rho_0} \tag{26}$$

and

$$c_s = \sqrt{\left(1 + D^2\cos^2\varphi\right)\left(1 + D^2\right)^{-2/3}\mu/\rho_0}, \tag{27}$$

where the propagation direction is defined as $\vec{n} = (\cos\varphi, \sin\varphi, 0)$. Hence, refraction angles of P-and S-waves are

$$\tan\theta_p = \frac{\left(K + \mu/3 + \mu\left(1 + D^2\right)^{-2/3}\right)\tan\varphi}{K + \mu/3 + \mu\left(1 + D^2\right)^{1/3}} \tag{28}$$

and

$$\tan\theta_s = \frac{\tan\varphi}{1 + D^2}. \tag{29}$$

Remarkably, relations (26), (27), (28) and (29) approximately hold even for very compressible materials with $K/\mu \sim 1$ for the range of deformations and electric fields considered here. By making use of relations (26) and (27), the slowness curves of P-and S-waves for the ideal DE can be constructed. Fig. 2 (b) shows an example

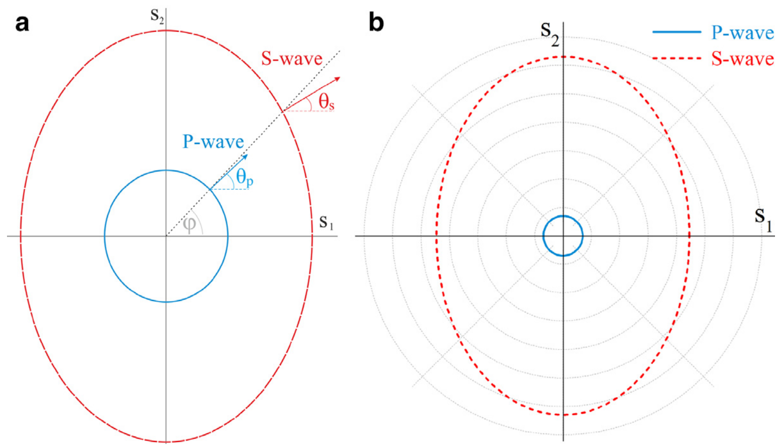

Fig. 2. (a) Schematic illustration of slowness curves for P-and S-waves in the DE subjected to an electric field. (b) Slowness curves of P-and S-waves for the ideal DE with $K/\mu = 50$ subjected to the electric excitation of $D = 1$. Slowness curves are constructed by using (26) and (27). Scale is 0.2 per division, and slowness curves are normalized by $\sqrt{\mu/\rho_0}$.

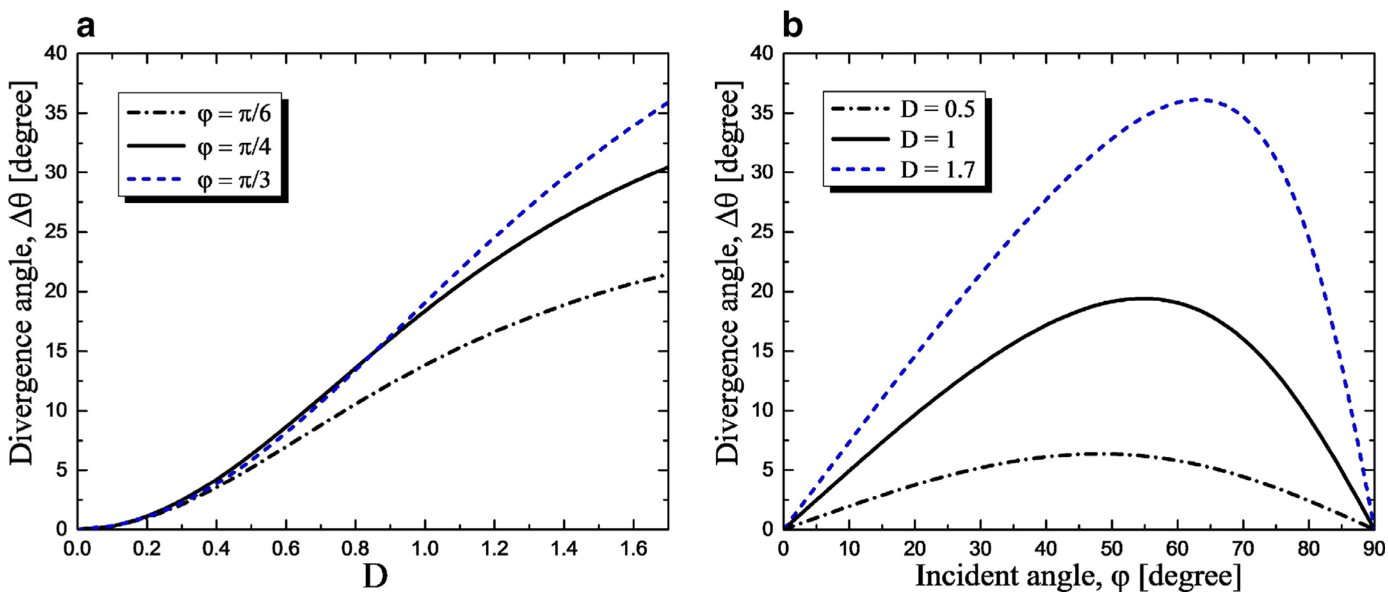

Fig. 3. Divergence angle as function of non-dimensional electric displacement – (a), and incident angle – (b) for the nearly incompressible neo-Hookean DE with $K/\mu = 300$.

of the slowness curves for an ideal DE with $K/\mu = 50$ subjected to the electric excitation of $D = 1$.

Fig. 3(a) shows that the divergence angle $\Delta\theta$ significantly depends on the value of an applied electric field. In particular, the divergence angle increases monotonically with an increase in the electric field until the limiting value of the electric field is reached ($D = \sqrt{3}$). Fig. 3(b) shows the dependence of the divergence angle $\Delta\theta$ on the incident angle φ. We observe that the divergence angle $\Delta\theta$ has a maximum for a certain incident angle φ_0 depending on the applied electric field. The incident angle φ_0 corresponding to the maximal divergence angle is given by

$$\tan\varphi_0 = \sqrt{\frac{\alpha\left(\alpha\mu^3(\alpha+27) + 3D^2\alpha_1\mu(\alpha_1 - 3\mu) + \zeta\right)}{\mu^3\left(\alpha^2+27\right) + \zeta}}, \qquad (30)$$

where $\alpha = 1 + D^2$, $\alpha_1 = \alpha^{2/3}(3K + \mu)$ and $\zeta = 9K\alpha^2\left(\mu^2 + 3K(K+\mu)\right)$. The maximal angle, φ_0, monotonically increases with an increase in the electric field. Note that for $\mu/K \ll 1$, $\varphi_0 = \arccos\left(2 + D^2\right)^{-1/2}$.

Next we consider the influence of the material compressibility on the elastic wave propagation in DEs. It has been recently shown that for highly compressible material (in the absence of an electric field) the phase velocity of the longitudinal wave depends significantly on the direction of wave propagation and applied deformation (Galich and Rudykh, 2015b). Here, we also observe a strong dependence of the P-wave velocity on the direction of wave propagation and the deformation induced by an electric field. An increase in the material compressibility parameter μ/K results in a more pronounced influence of electrostatically induced deformation on elastic waves. In particular, the slowness curves of P-wave evolve from circle to ellipse shape with an increase in electric field. Thus, refraction angle of P-wave differs from the incident angle, namely P-wave refracts along with S-wave. Fig. 4 schematically illustrates the phenomenon in compressible materials. The dependence of the divergence angle on compressibility for different values of the electrostatic excitation is presented in Fig. 5. Clearly, an increase in material compressibility weakens the disentangling phenomenon.

3.2. Enriched electroactive material model

Motivated by the experimental observations (Wissler and Mazza, 2007; Li et al., 2011), in this section we investigate elastic wave propagation in DEs described by an enriched electroactive material model (13). The model is similar to that considered by

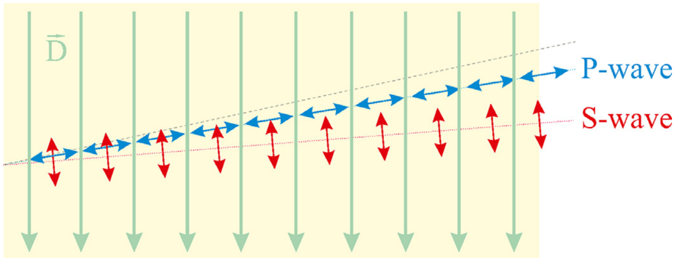

Fig. 4. Schematics of the splitting of P-and S-waves in the compressible neo-Hookean DE. P-and S-waves unidirectionally refract from the initial direction of propagation, however, their refraction angles are different.

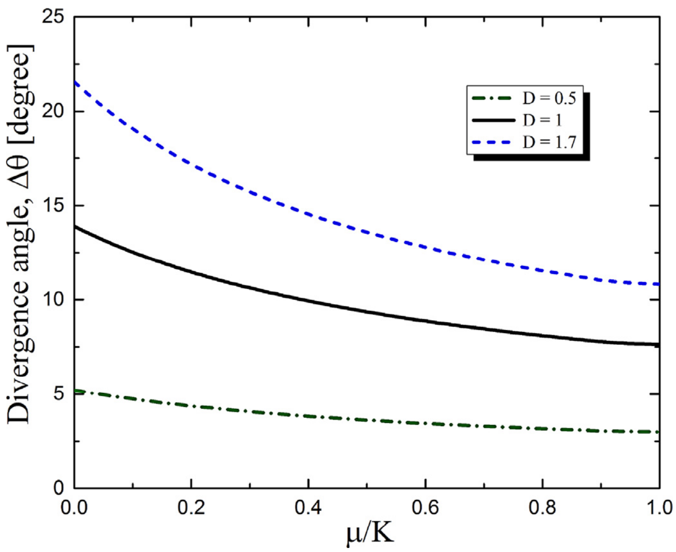

Fig. 5. Divergence angle as function of material compressibility for the ideal neo-Hookean DE subjected to different levels of electrostatic excitation, $\varphi = \pi/6$.

Table 1
Material constants of DE model (13).

Reference	γ_0	γ_1	γ_2
Ideal DE (Zhao et al., 2007)	0	1	0
Wissler and Mazza (2007)	0.00104	1.14904	−0.15008
Li et al. (2011)	0.00458	1.3298	−0.33438

Gei et al. (2014). To allow for the investigation of pressure waves, we extend the model to capture the compressibility effects. Table 1 summarizes the parameters of the material model (13) for different experimental data (Wissler and Mazza, 2007; Li et al., 2011).

In the case when $\gamma_0 \neq 0$, $\gamma_2 \neq 0$, and the deformation gradient identical to (25), and $\vec{n} = \vec{e}_1$, the expressions for phase velocities take the following form

$$c_p = \sqrt{\left((K - 2\mu/3)\lambda^2\tilde{\lambda}^4 + \left(1 + \tilde{\lambda}^2\right)\mu\right)/\rho_0} \quad (\vec{m} = \vec{e}_1), \tag{31}$$

$$c_s = \sqrt{\left(\gamma_2 D^2 \lambda + \tilde{\lambda}^2\right)\mu/\rho_0} \quad (\vec{m} = \vec{e}_2) \tag{32}$$

and

$$c_s = \tilde{\lambda}\sqrt{\mu/\rho_0} \quad (\vec{m} = \vec{e}_3). \tag{33}$$

For incompressible materials $\tilde{\lambda} = \lambda^{-1/2}$, and the stretch ratio λ can be determined by solving the following polynomial equation

$$\lambda^3\left(1 + D^2\left(\gamma_1 + 2\gamma_2\lambda^2\right)\right) = 1. \tag{34}$$

Hence, the phase velocity of the in-plane shear wave (with polarization $\vec{m} = \vec{e}_2$) explicitly depends on the electric field in contrast to the result $(24)_2$ for the ideal DE model. Fig. 6 shows the

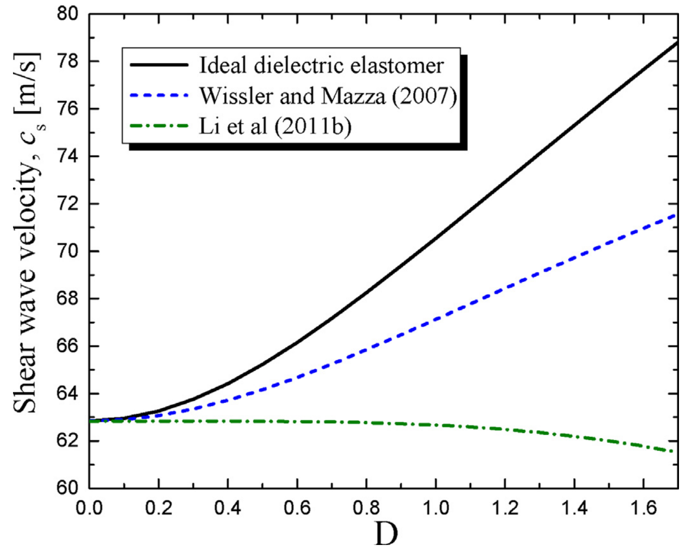

Fig. 6. Phase velocity of in-plane shear wave as functions of non-dimensional electric displacement for ideal and enriched DE models, $\varphi = 0$.

phase velocity of the in-plane shear wave as a function of the non-dimensional electrostatic excitation for the ideal and enriched DE models. One can see that the consideration of the I_{4e} and I_{6e} invariants strongly influences the in-plane shear wave velocity. In particular, the increase in phase velocity of the in-plane shear wave is less prominent (dashed blue curve in Fig. 6) as compared with the ideal DE model result; moreover, the velocity may even decrease with an increase in the electric field (see the example for the particular material denoted by the dot-dashed green curve in Fig. 6), while for the ideal DE model the velocity always increases. These differences indeed affect the splitting mechanism and, thus, different results are produced by these material models. Fig. 7 illustrates the difference in the divergence angles for the ideal and enriched DE models. In particular, Fig. 7(a) shows that the divergence angle $\Delta\theta$ is smaller than it is predicted by the ideal DE model. Moreover, for Li et al. experimental data, the divergence angle $\Delta\theta$ decreases with an increase in the electric field after a certain level of the applied voltage is reached. Fig. 7(b) shows that the divergence angle $\Delta\theta$ has a maximum for a certain incident angle φ_1. Moreover, the incident angle φ_1, producing the maximum divergence angle, varies for different materials.

Although in this work we perform a fully electromechanical coupling analysis, it is possible to employ only a purely mechanical analysis of wave propagation in non-linear electroelastic solids. In that case the contribution of the electroelastic moduli tensors $\mathcal{M}$ and $\mathbf{K}$ is neglected, and only terms of the tensor $\mathbb{C}$ contribute to the generalized acoustic tensor. Remarkably, this approximation yields very close results for the phase velocity of pressure wave as the fully electromechanically coupled analysis; moreover, the resulting expressions for the phase velocities of the shear waves are identical in both analyzes. For example, for the deformation gradient (25), $\vec{n} = \vec{e}_1$ and $\vec{D}_0 = D\sqrt{\mu\epsilon}\vec{e}_2$, the *classic* acoustic tensor takes the form

$$\mathbf{Q} = \mathbf{Q}_{elas} + \mu D^2(\gamma_0 J^{-2} + \gamma_1\tilde{\lambda}^{-4} + \gamma_2\lambda^2\tilde{\lambda}^{-4})\vec{e}_1 \otimes \vec{e}_1 + \mu\gamma_2 D^2\tilde{\lambda}^{-2}\vec{e}_2 \otimes \vec{e}_2. \tag{35}$$

It is easy to see that the resulting expressions for the phase velocities of S-waves are the same as given by expressions (32) and (33), and the corresponding expression for the phase velocity of P-wave has the form

$$c_p = \sqrt{\mu\left(1 + \tilde{\lambda}^2 + (K/\mu - 2/3)\lambda^2\tilde{\lambda}^4 + D^2(\gamma_0\lambda^{-2} + \gamma_1 + \gamma_2\lambda^2)\tilde{\lambda}^{-4}\right)/\rho_0}. \tag{36}$$

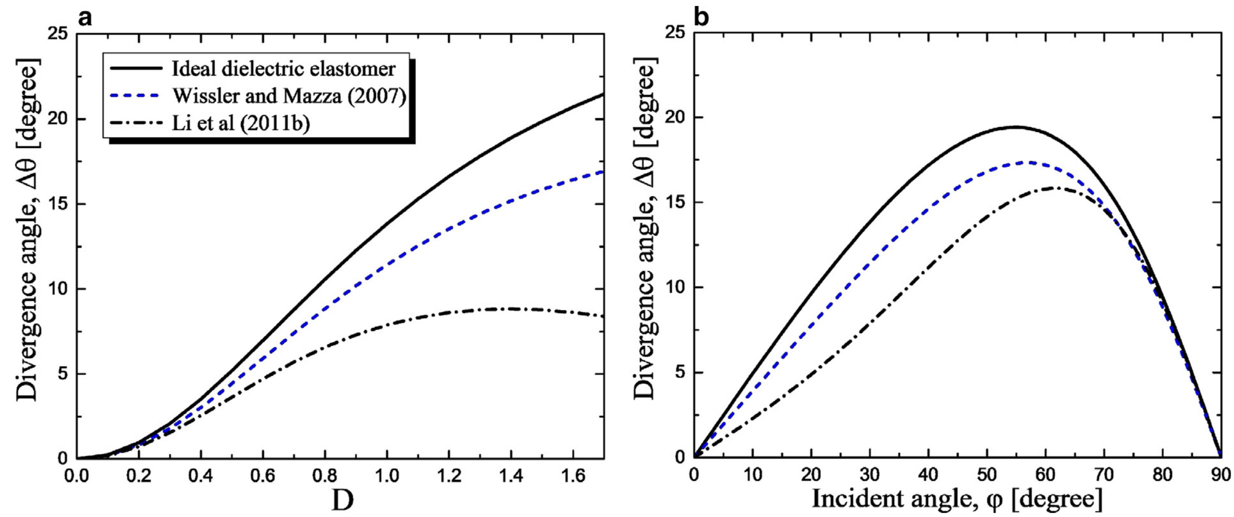

Fig. 7. Divergence angle as function of non-dimensional electric displacement for $\varphi = \pi/6$ (a) and incident angle for $D = 1$ (b) in the nearly incompressible neo-Hookean DE with $K/\mu = 300$.

Expression (36) for the P-wave velocity differs from (31) by the additional term containing the electric displacement magnitude. However, according to our observations for $K/\mu \gtrsim 100$, this term can be neglected for small and moderate levels of electric displacement.

4. Concluding remarks

In this paper, we considered pressure (P-) and shear (S-) elastic waves propagating in soft DEs subjected to finite deformations in the presence of an electric field. To allow for the consideration of P-wave propagation, we utilized the ideal and enriched material models accounting for the *compressibility* effects. Explicit expressions for the generalized acoustic tensor and phase velocities of elastic waves for DEs subjected to an electric field were presented. We found that, for the ideal DE model, the elastic wave propagation is explicitly independent of an applied electric field, while it is influenced through the deformation induced via bias electric field; this is despite the fact that all electroelastic moduli tensors explicitly depend on the applied electric field. However, for the enriched material model, including all three electroelastic invariants I_{4e}, I_{5e} and I_{6e}, elastic wave propagation explicitly depends on the applied electric field; in particular, the phase velocity of the in-plane shear wave decreases when an electric field is applied.

These findings were applied to explore the phenomenon of disentangling P-and S-elastic waves in DEs by an electric field. We showed that the divergence angle between P-and S-waves strongly depends on the value of the applied electric field and direction of wave propagation. Moreover, we found that an increase in the material compressibility weakens the separation of P-and S-waves. This is due to the fact that the P-wave also refracts (in the same direction as the S-wave) from the initial direction of wave propagation, while for nearly incompressible materials the change in the P-wave direction is negligible. The phenomenon can be used to manipulate elastic waves by a bias electrostatic field; this can be beneficial for applications in small length-scale devices, such as micro-electromechanical systems, where an electric field is the preferred control parameter. Thanks to the mathematical similarities in the description of electro- and magneto-active materials, the disentangling phenomenon can be utilized to control P-and S-waves in magnetorheological elastomers by applying an external magnetic field.

Acknowledgments

This research was supported by the ISRAEL SCIENCE FOUNDATION (grants 1550/15 and 1973/15). SR gratefully acknowledges the support of Taub Foundation through the Horev Fellowship – Leaders in Science and Technology.

Appendix A. Notation of tensor isomers

To achieve a more compact representation of the results, we have used the notation of isomers firstly introduced by Ryzhak (1993); Nikitin and Ryzhak (2008). Let $\mathcal{S}$ be a third-rank tensor with the following representation as the sum of a certain number of triads:

$$\mathcal{S} = \vec{a}_1 \otimes \vec{a}_2 \otimes \vec{a}_3 + \vec{b}_1 \otimes \vec{b}_2 \otimes \vec{b}_3 + \cdots \tag{A.1}$$

Let (ikj) be some permutation of the set (123). Then the isomer $\mathcal{S}^{(ikj)}$ is defined to be the third-rank tensor determined by the relation

$$\mathcal{S}^{(ikj)} = \vec{a}_i \otimes \vec{a}_k \otimes \vec{a}_j + \vec{b}_i \otimes \vec{b}_k \otimes \vec{b}_j + \cdots \tag{A.2}$$

Analogously, we can define isomers for higher-rank tensors. For example, if $\mathcal{S} = \vec{b} \otimes \mathbf{I}$, where $\vec{b}$ is an arbitrary vector and $\mathbf{I}$ is the unit tensor, then $\mathcal{S}^{(231)} = \mathcal{S}^{(321)} = \mathbf{I} \otimes \vec{b}$ and $\mathcal{S}^{(132)} = \mathcal{S}$. If $\mathbb{S} = \mathbf{M} \otimes \mathbf{N}$, where $\mathbf{N}$ and $\mathbf{M}$ are arbitrary second-rank tensors, then $\mathbb{S}^{(3412)} = \mathbf{N} \otimes \mathbf{M}$.

Appendix B. Components of the electroelastic moduli and generalized acoustic tensors

Here we introduce the following notations

$$\begin{aligned}
L_{ab} &= \vec{a} \cdot \mathbf{L} \cdot \vec{b},\, L_{ab}^{(2)} = \vec{a} \cdot \mathbf{L}^2 \cdot \vec{b},\, \mathbf{L}^2 = \mathbf{L} \cdot \mathbf{L}, \\
L_{ab}^{(-1)} &= \vec{a} \cdot \mathbf{L}^{-1} \cdot \vec{b},\, L_{ab}^{(-2)} = \vec{a} \cdot \mathbf{L}^{-2} \cdot \vec{b},\, \mathbf{L}^{-2} = \mathbf{L}^{-1} \cdot \mathbf{L}^{-1}, \\
L_{ab}^{(3)} &= \vec{a} \cdot \mathbf{L}^3 \cdot \vec{b},\, \mathbf{L}^3 = \mathbf{L}^2 \cdot \mathbf{L},\, L_{ab}^{(-3)} = \vec{a} \cdot \mathbf{L}^{-3} \cdot \vec{b}, \\
\mathbf{L}^{-3} &= \mathbf{L}^{-2} \cdot \mathbf{L}^{-1},\, \vec{a} \otimes \vec{b}^s = \frac{1}{2}\left(\vec{a} \otimes \vec{b} + \vec{b} \otimes \vec{a}\right), \\
a_b &= \vec{a} \cdot \vec{b},\, a_b^2 = (a_b)^2,
\end{aligned} \tag{B.1}$$

where $\mathbf{L}$ is an arbitrary second-rank tensor, $\vec{a}$ and $\vec{b}$ are arbitrary vectors.

$$\mathbb{C}_{4e} = B_{DD}^{-1}(\mathbf{I} \otimes \mathbf{I} + \mathbf{I} \otimes \mathbf{I}^{(1342)}),$$

$$\mathbb{C}_{5e} = 2(\vec{D} \otimes \mathbf{I} \otimes \vec{D}^{(2134)} - \vec{D} \otimes \vec{D} \otimes \mathbf{I} - \mathbf{I} \otimes \vec{D} \otimes \vec{D})$$

$$
\begin{aligned}
&+D_D(\mathbf{I}\otimes\mathbf{I}+\mathbf{I}\otimes\mathbf{I}^{(1342)}),\\
\mathbb{C}_{6e} =\ & 2(\vec{D}\otimes\mathbf{I}\otimes(\mathbf{B}\cdot\vec{D})^{(2134)}+\mathbf{B}\otimes\vec{D}\otimes\vec{D}^{(1432)}\\
&+\vec{D}\otimes\mathbf{B}\otimes\vec{D}^{(2134)}+(\mathbf{B}\cdot\vec{D})\otimes\mathbf{I}\otimes\vec{D}^{(2134)}\\
&+\vec{D}\otimes\vec{D}\otimes\mathbf{B}^{(1324)}+\vec{D}\otimes\mathbf{B}\otimes\vec{D}\\
&-\mathbf{I}\otimes(\mathbf{B}\cdot\vec{D})\otimes\vec{D}-\mathbf{I}\otimes\vec{D}\otimes(\mathbf{B}\cdot\vec{D})\\
&-\vec{D}\otimes(\mathbf{B}\cdot\vec{D})\otimes\mathbf{I}-(\mathbf{B}\cdot\vec{D})\otimes\vec{D}\otimes\mathbf{I})\\
&+B_{DD}(\mathbf{I}\otimes\mathbf{I}+\mathbf{I}\otimes\mathbf{I}^{(1342)}).
\end{aligned}\tag{B.2}
$$

$$
\begin{aligned}
\mathbf{Q}_{4e} =\ & 2\ B_{DD}^{(-1)}\vec{n}\otimes\vec{n},\\
\mathbf{Q}_{5e} =\ & 2((D_D+D_n^2)\vec{n}\otimes\vec{n}+D_n^2\hat{\mathbf{I}}-2D_n\vec{D}\otimes\vec{n}^s),\\
\mathbf{Q}_{6e} =\ & 2((2B_{Dn}D_n+B_{DD})\vec{n}\otimes\vec{n}+2B_{Dn}D_n\hat{\mathbf{I}}\\
&-2B_{Dn}\vec{D}\otimes\vec{n}^s+D_n^2\mathbf{B}+2D_n(\mathbf{B}\cdot\vec{n})\otimes\vec{D}^s\\
&-2D_n(\mathbf{B}\cdot\vec{D})\otimes\vec{n}^s+B_{nn}\vec{D}\otimes\vec{D}).
\end{aligned}\tag{B.3}
$$

$$
\begin{aligned}
\mathcal{M}_{4e} =\ & -2\mathbf{I}\otimes(\mathbf{B}^{-1}\cdot\vec{D}),\\
\mathcal{M}_{5e} =\ & 2(\vec{D}\otimes\mathbf{I}+\vec{D}\otimes\mathbf{I}^{(213)}-\mathbf{I}\otimes\vec{D}),\\
\mathcal{M}_{6e} =\ & 2(\vec{D}\otimes\mathbf{B}+\vec{D}\otimes\mathbf{B}^{(213)}+(\mathbf{B}\cdot\vec{D})\otimes\mathbf{I}\\
&+(\mathbf{B}\cdot\vec{D})\otimes\mathbf{I}^{(213)}-\mathbf{I}\otimes(\mathbf{B}\cdot\vec{D})).
\end{aligned}\tag{B.4}
$$

$$
\begin{aligned}
\mathbf{R}_{4e} =\ & -2\vec{n}\otimes(\mathbf{B}^{-1}\cdot\vec{D}),\\
\mathbf{R}_{5e} =\ & 2(D_n\mathbf{I}+\vec{D}\otimes\vec{n}-\vec{n}\otimes\vec{D}),\\
\mathbf{R}_{6e} =\ & 2(D_n\mathbf{B}+\vec{D}\otimes(\mathbf{B}\cdot\vec{n})+B_{Dn}\mathbf{I}\\
&+(\mathbf{B}\cdot\vec{D})\otimes\vec{n}-\vec{n}\otimes(\mathbf{B}\cdot\vec{D})).
\end{aligned}\tag{B.5}
$$

$$
\begin{aligned}
\eta =\ & \gamma_0^2\left(2B_{nn}^{(-2)}-\mathbf{B}^{-1}:\mathbf{B}^{-1}-(B_{nn}^{(-1)})^2\right)\\
&+\gamma_2^2\left(2B_{nn}^{(2)}-\mathbf{B}:\mathbf{B}-(B_{nn})^2\right)\\
&+\left(\gamma_0\left(\mathbf{I}:\mathbf{B}^{-1}-B_{nn}^{(-1)}\right)+\gamma_1\right)^2+(\gamma_2\beta+\gamma_1)^2\\
&+2\gamma_0\gamma_2\left((\mathbf{I}:\mathbf{B}^{-1})\beta-I_1B_{nn}^{(-1)}-1\right)
\end{aligned}\tag{B.6}
$$

$$
\begin{aligned}
\mathbf{A}_e =\ & a_1\vec{n}\otimes\vec{n}+a_2\mathbf{I}+a_3\vec{D}\otimes\vec{D}+a_4\vec{n}\otimes\vec{D}^s+a_5\mathbf{B}+a_6(\mathbf{B}\cdot\vec{n})\otimes\vec{D}^s\\
&+a_7(\mathbf{B}\cdot\vec{D})\otimes\vec{n}^s+a_8(\mathbf{B}\cdot\vec{n})\otimes\vec{n}^s+a_9\mathbf{B}^2+a_{10}(\mathbf{B}^2\cdot\vec{n})\otimes\vec{D}^s\\
&+a_{11}(\mathbf{B}^2\cdot\vec{D})\otimes\vec{n}^s+a_{12}(\mathbf{B}^2\cdot\vec{n})\otimes\vec{n}^s+a_{13}(\mathbf{B}\cdot\vec{n})\otimes(\mathbf{B}\cdot\vec{n})\\
&+a_{14}\mathbf{B}^3+a_{15}(\mathbf{B}^3\cdot\vec{n})\otimes\vec{D}^s+a_{16}(\mathbf{B}^3\cdot\vec{D})\otimes\vec{n}^s\\
&+a_{17}(\mathbf{B}^2\cdot\vec{n})\otimes(\mathbf{B}\cdot\vec{n})^s+a_{18}\mathbf{B}^{-1}+a_{19}(\mathbf{B}^{-1}\cdot\vec{n})\otimes\vec{n}^s\\
&+a_{20}(\mathbf{B}^{-1}\cdot\vec{n})\otimes\vec{D}^s+a_{21}(\mathbf{B}^{-1}\cdot\vec{D})\otimes\vec{n}^s\\
&+a_{22}(\mathbf{B}^{-1}\cdot\vec{n})\otimes(\mathbf{B}\cdot\vec{n})^s+a_{23}(\mathbf{B}^{-2}\cdot\vec{D})\otimes\vec{n}^s,
\end{aligned}\tag{B.7}
$$

where

$$
\begin{aligned}
a_1 =\ & \gamma_0^3\left(\left(B_{DD}^{(-2)}-(B_{Dn}^{(-1)})^2\right)\mathbf{I}:\mathbf{B}^{-1}-B_{nn}^{(-1)}B_{DD}^{(-2)}-B_{DD}^{(-3)}\right.\\
&\left.+2B_{Dn}^{(-1)}B_{Dn}^{(-2)}\right)+\gamma_1^3D_D\\
&+\gamma_2^3\left(\beta B_{DD}^{(2)}-B_{DD}^{(3)}\right)+2\gamma_0\gamma_1\gamma_2\left(\beta B_{DD}^{(-1)}+B_{Dn}B_{Dn}^{(-1)}\right.\\
&\left.+\beta_4B_{DD}-D_D\right)\\
&+\gamma_0\gamma_1^2\left(\beta_4D_D+B_{DD}^{(-1)}\right)+\gamma_0\gamma_2^2\left(\beta_4B_{DD}^{(2)}-3B_{DD}+2\beta D_D\right.\\
&\left.+2B_{Dn}^{(-1)}B_{Dn}^{(2)}\right)\\
&+\gamma_1\gamma_0^2\left(2\beta_4B_{DD}^{(-1)}-B_{DD}^{(-2)}+(B_{Dn}^{(-1)})^2\right)+\gamma_1\gamma_2^2\left(2\beta B_{DD}-B_{DD}^{(2)}\right)\\
&+\gamma_2\gamma_0^2\left(\beta B_{DD}^{(-2)}-3B_{DD}^{(-1)}+2\beta_4D_D+B_{Dn}^{(-1)}\left(2D_n-I_1B_{Dn}^{(-1)}\right)\right)\\
&+\gamma_2\gamma_1^2(\beta D_D+B_{DD}),\\
a_2 =\ & \gamma_1^3D_n^2+\gamma_2^3\beta(B_{Dn})^2+2\gamma_0\gamma_1\gamma_2D_n(\beta_4B_{Dn}-D_n)+\gamma_0\gamma_1^2\beta_4D_n^2\\
&+\gamma_0\gamma_2^2(\beta_4B_{Dn}-2D_n)B_{Dn}+\gamma_1\gamma_2^2B_{Dn}(B_{Dn}+2\beta D_n)\\
&+\gamma_2\gamma_1^2(\beta D_n+2B_{Dn})D_n,\\
a_3 =\ & \gamma_2^2\left(\gamma_2\left(I_1\left(B_{nn}^{(2)}-(B_{nn})^2\right)+B_{nn}B_{nn}^{(2)}-B_{nn}^{(3)}\right)\right.\\
&+\gamma_0\left(B_{nn}-B_{nn}^{(-1)}B_{nn}^{(2)}+(\mathbf{I}:\mathbf{B}^{-1})\left(B_{nn}^{(2)}-(B_{nn})^2\right)\right)\\
&\left.+\gamma_1\left(B_{nn}^{(2)}-(B_{nn})^2\right)\right),\\
a_4 =\ & 2\left(\gamma_0\gamma_1\gamma_2(D_n-2\beta_4B_{Dn})-\gamma_1^3D_n-\gamma_2^3\left(I_1B_{Dn}^{(2)}-B_{Dn}^{(3)}\right)\right.\\
&-\gamma_0\gamma_1^2\beta_4D_n\\
&+\gamma_0\gamma_2^2\left(3B_{Dn}-\beta_4B_{Dn}^{(2)}+I_1\left(B_{Dn}^{(-1)}B_{nn}-2D_n\right)\right.\\
&\left.+D_nB_{nn}-B_{Dn}^{(-1)}B_{nn}^{(2)}\right)+\gamma_1\gamma_2^2B_{Dn}(B_{nn}-2I_1)\\
&+\gamma_2\gamma_0^2\left(B_{nn}\left(B_{Dn}^{(-1)}(\mathbf{I}:\mathbf{B}^{-1})-B_{Dn}^{(-2)}\right)-2D_n\beta_4\right)\\
&\left.-\gamma_2\gamma_1^2(\beta D_n+2B_{Dn})\right),\\
a_5 =\ & \gamma_2\left(\gamma_2^2B_{Dn}(2D_n\beta-B_{Dn})+2\gamma_0\gamma_1\beta_4D_n^2\right.\\
&\left.+\gamma_0\gamma_2D_n(2\beta_4B_{Dn}-D_n)+2\gamma_1\gamma_2\beta D_n^2+\gamma_1^2D_n^2\right),
\end{aligned}\tag{B.8}
$$

$$
\begin{aligned}
a_6 =\ & 2\gamma_2\left(\gamma_2^2\left(D_nB_{nn}^{(2)}+I_1(B_{Dn}-D_nB_{nn})\right)+\gamma_0\gamma_1\beta_4D_n\right.\\
&+\gamma_0\gamma_2\left((\mathbf{I}:\mathbf{B}^{-1})(B_{Dn}-D_nB_{nn})-B_{nn}^{(-1)}B_{Dn}\right)\\
&\left.+\gamma_1\gamma_2(B_{Dn}+\beta D_n)+\gamma_1^2D_n\right),\\
a_7 =\ & -2\gamma_2\left(\gamma_2^2\beta B_{Dn}+2\gamma_0\gamma_1\beta_4D_n+\gamma_0\gamma_2(\beta_4B_{Dn}-2D_n)\right.\\
&\left.+2\gamma_1\gamma_2\beta D_n+\gamma_1^2D_n\right),\\
a_8 =\ & 2\gamma_2\left(\gamma_0\gamma_2\left(B_{Dn}^{(-1)}(I_1D_n-B_{Dn})-D_n^2\right)\right.\\
&+D_n\left(\gamma_0^2\left(B_{Dn}^{(-1)}(\mathbf{I}:\mathbf{B}^{-1})-B_{Dn}^{(-2)}\right)-\gamma_2^2B_{Dn}^{(2)}\right.\\
&\left.\left.-\gamma_0\gamma_1B_{Dn}^{(-1)}-\gamma_1\gamma_2B_{Dn}\right)\right),\\
a_9 =\ & \gamma_2^2D_n(\gamma_2(\beta D_n-2B_{Dn})+D_n(\gamma_0\beta_4-\gamma_1)),\\
a_{10} =\ & 2\gamma_2^2(\gamma_2(I_1D_n-B_{Dn})+\gamma_0\beta_4D_n),\\
a_{11} =\ & 2\gamma_2^2(\gamma_2(B_{Dn}-\beta D_n)-D_n(\gamma_0\beta_4-\gamma_1)),\\
a_{12} =\ & -2\gamma_0\gamma_2^2D_nB_{Dn}^{(-1)},\\
a_{13} =\ & \gamma_2^2D_n\left(\gamma_2(2B_{Dn}-I_1D_n)+\gamma_1D_n-\gamma_0D_n(\mathbf{I}:\mathbf{B}^{-1})\right),\\
a_{14} =\ & -\gamma_2^3D_n^2,\ a_{15}=-2\gamma_2^3D_n,\ a_{16}=-a_{15},\ a_{17}=-2a_{14},\\
a_{18} =\ & -\gamma_0(\gamma_1D_n+\gamma_2B_{Dn})^2,\ a_{19}=-2\gamma_0^2B_{Dn}^{(-1)}(\gamma_1D_n+\gamma_2B_{Dn}),\\
a_{20} =\ & 2\gamma_0\gamma_2B_{nn}(\gamma_1D_n+\gamma_2B_{Dn}),\\
a_{21} =\ & 2\gamma_0(\gamma_2\gamma_0(D_n-\beta_4B_{Dn})-\gamma_2\beta(\gamma_1D_n+\gamma_2B_{Dn})-\gamma_1\gamma_0\beta_4D_n),\\
a_{22} =\ & 2\gamma_0\gamma_2D_n(\gamma_1D_n+\gamma_2B_{Dn}),\ a_{23}=2\gamma_0^2(\gamma_1D_n+\gamma_2B_{Dn}),\\
\beta =\ & I_1-B_{nn}\quad\text{and}\quad\beta_4=\mathbf{I}:\mathbf{B}^{-1}-B_{nn}^{(-1)}.
\end{aligned}\tag{B.9}
$$

References

Aboudi, J., 2015. Micro-electromechanics of soft dielectric matrix composites. Int. J. Solids Struct. 64, 30–41.

Achenbach, J.D., 1973. Wave Propagation in Elastic Solids. Applied Mathematics and Mechanics. North-Holland Publishing Company.

Bar-Cohen, Y., 2002. Electroactive polymers as artificial muscles: A review. J. Spacecr. Rockets 39 (6), 822–827.

Bortot, E., Denzer, R., Menzel, A., Gei, M., 2016. Analysis of viscoelastic soft dielectric elastomer generators operating in an electrical circuit. Int. J. Solids Struct. 78-79, 205–215.

Brochu, P., Pei, Q., 2010. Advances in dielectric elastomers for actuators and artificial muscles. Macromol. Rapid Commun. 31 (1), 10–36.

Cao, C., Zhao, X., 2013. Tunable stiffness of electrorheological elastomers by designing mesostructures. Appl. Phys. Lett. 103, 041901.

Carpi, F., De Rossi, D., Kornbluh, R., Pelrine, R.E., Sommer-Larsen, P., 2011. Dielectric Elastomers as Electromechanical Transducers: Fundamentals, Materials, Devices, Models and Applications of an Emerging Electroactive Polymer Technology. Elsevier Science.

Chatzigeorgiou, G., Javili, A., Steinmann, P., 2015. Interface properties influence the effective dielectric constant of composites. Philos. Mag. 95 (28–30), 3402–3412.

Chen, W., Dai, H., 2012. Waves in pre-stretched incompressible soft electroactive cylinders: exact solution. Acta Mech. Solida Sinica 25 (5), 530–541.

Cohen, N., deBotton, G., 2014. Multiscale analysis of the electromechanical coupling in dielectric elastomers. Eur. J. Mech. A/Solids 48, 48–59.

Cohen, N., Menzel, A., deBotton, G., 2016. Towards a physics-based multiscale modelling of the electro-mechanical coupling in electro-active polymers. Proc. R. Soc. A 472, 20150462.

Destrade, M., Ogden, R.W., 2011. On magneto-acoustic waves in finitely deformed elastic solids. Math. Mech. Solids 16, 594–604.

Dorfmann, A., Ogden, R.W., 2005. Nonlinear electroelasticity. Acta Mech. 174, 167–183.

Dorfmann, A., Ogden, R.W., 2010. Electroelastic waves in a finitely deformed electroactive material. J. Appl. Math. 75, 603–636.

Galich, P.I., Rudykh, S., 2015a. Comment on "disentangling longitudinal and shear elastic waves by neo-hookean soft devices" [appl. phys. lett. 106, 161903 (2015)]. Appl. Phys. Lett. 107 (5), 056101.

Galich, P.I., Rudykh, S., 2015b. Influence of stiffening on elastic wave propagation in extremely deformed soft matter: from nearly incompressible to auxetic materials. Extreme Mech. Lett. 4, 156–161.

Galipeau, E., Rudykh, S., deBotton, G., Ponte Castañeda, P., 2014. Magnetoactive elastomers with periodic and random microstructures. Int. J. Solids Struct. 51, 3012–3024.

Gei, M., Colonnelli, S., Springhetti, R., 2014. The role of electrostriction on the stability of dielectric elastomer actuators. Int. J. Solids Struct. 51 (3–4), 848–860.

Gei, M., Roccabianca, S., Bacca, M., 2011. Controlling bandgap in electroactive polymer-based structures. IEEE/ASME Trans. Mechatron. 16 (1), 102–107.

Hossain, M., Vu, D.K., Steinmann, P., 2015. A comprehensive characterization of the electro-mechanically coupled properties of VHB 4910 polymer. Arch. Appl. Mech. 85 (4), 523–537.

Huang, C., Zhang, Q.M., deBotton, G., Bhattacharya, K., 2004. All-organic dielectric-percolative three-component composite materials with high electromechanical response. Appl. Phys. Lett. 84 (22), 4391–4393.

Itskov, M., Khiêm, V.N., 2014. A polyconvex anisotropic free energy function for electro-and magneto-rheological elastomers. Math. Mech. Solids 1081286514555140.

Jabareen, M., 2015. On the modeling of electromechanical coupling in electroactive polymers using the mixed finite element formulation. Procedia IUTAM 12, 105–115.

Keip, M.A., Steinmann, P., Schröder, J., 2014. Two-scale computational homogenization of electro-elasticity at finite strains. Comput. Methods Appl. Mech. Eng. 278, 62–79.

Kornbluh, R., Pelrine, R., Prahlad, H., Wong-Foy, A., McCoy, B., Kim, S., Eckerle, J., Low, T., 2012. From boots to buoys: Promises and challenges of dielectric elastomer energy harvesting. In: Lenore, R. (Ed.), Electroactivity in Polymeric Materials. Springer, US, pp. 67–93.

Li, B., Chen, H., Qiang, J., Hu, S., Zhu, Z., Wang, Y., 2011. Effect of mechanical pre-stretch on the stabilization of dielectric elastomer actuation. J. Phys. D Appl. Phys. 44 (15), 155301.

Madsen, F.B., Yu, L., Daugaard, A.E., Hvilsted, S., Skov, A.L., 2014. Silicone elastomers with high dielectric permittivity and high dielectric breakdown strength based on dipolar copolymers. Polymer 55 (24), 6212–6219.

Maugin, G.A., 1985. Nonlinear Electromechanical Effects and Applications, 1. World Scientific.

Miehe, C., Vallicotti, D., Zäh, D., 2015. Computational structural and material stability analysis in finite electro-elasto-statics of electro-active materials. Int. J. Numer. Methods Eng. 102 (10), 1605–1637.

Nikitin, L.V., Ryzhak, E.I., 2008. On stability and instability of a compressed block pressed to a smooth basement. Mech. Solids 43 (4), 558–570.

O'Halloran, A., O'Malley, F., McHugh, P., 2008. A review on dielectric elastomer actuators, technology, applications, and challenges. J. Appl. Phys. 104 (7), 071101.

Ogden, R.W., 1997. Non-Linear Elastic Deformations. Dover Publications, New York.

Pelrine, R., Kornbluh, R., Pei, Q., Joseph, J., 2000. High-speed electrically actuated elastomers with strain greater than 100. Science 287 (5454), 836–839.

Rogers, J.A., 2013. A Clear Advance in Soft Actuators. Science 341 (6149), 968–969.

Rudykh, S., Bertoldi, K., 2013. Stability of anisotropic magnetorheological elastomers in finite deformations: a micromechanical approach. J. Mech. Phys. Solids 61, 949–967.

Rudykh, S., Bhattacharya, K., deBotton, G., 2012. Snap-through actuation of thick--wall electroactive balloons. Int. J. Nonlinear Mech. 47, 206–209.

Rudykh, S., Bhattacharya, K., deBotton, G., 2014. Multiscale instabilities in soft heterogeneous dielectric elastomers. Proc. R. Soc. A 470, 20130618.

Rudykh, S., Boyce, M.C., 2014. Transforming wave propagation in layered media via instability-induced interfacial wrinkling. Phys. Rev. Lett. 112, 034301.

Rudykh, S., deBotton, G., 2011. Stability of anisotropic electroactive polymers with application to layered media. Z. Angew. Math. Phys. 62, 1131–1142.

Rudykh, S., Lewinstein, A., Uner, G., deBotton, G., 2013. Analysis of microstructural induced enhancement of electromechanical coupling in soft dielectrics. Appl. Phys. Lett. 102, 151905.

Ryzhak, E.I., 1993. On stable deformation of unstable materials in a rigid triaxial testing machine. J. Mech. Phys. Solids 41 (8), 1345–1356.

Sarvazyan, A., Rudnenko, O., Swanson, S., Fowlkes, J., Emelianov, S., 1998. Shear wave elasticity imaging: a new ultrasonic technology of medical diagnostics. Ultrasound Med. Biol. 24 (9), 1419–1435.

Shmuel, G., Gei, M., deBotton, G., 2012. The rayleigh-lamb wave propagation in dielectric elastomer layers subjected to large deformations. Int. J. Nonlinear Mech. 47 (2), 307–316.

Siboni, M.H., Avazmohammadi, R., Ponte-Castañeda, P., 2014. Electromechanical instabilities in fiber-constrained, dielectric-elastomer composites subjected to all-around dead-loading. Math. Mech. Solids 1081286514551501.

Spinelli, S.A., Lopez-Pamies, O., 2015. Some simple explicit results for the elastic dielectric properties and stability of layered composites. Int. J. Eng. Sci. 88, 15–28.

Suo, Z., 2010. Theory of dielectric elastomers. Acta Mech. Solida Sinica 23 (6), 549–578.

Suo, Z., Zhao, X., Greene, W.H., 2008. A nonlinear field theory of deformable dielectrics. J. Mech. Phys. Solids 56, 467–486.

Toupin, R.A., 1956. The elastic dielectric. J. Ration. Mech. Anal. 5, 849–915.

Toupin, R.A., 1963. A dynamical theory of elastic dielectrics. Int. J. Eng. Sci. 1, 101–126.

Volokh, K.Y., 2012. On electromechanical coupling in elastomers. J. Appl. Mech. 79 (4), 044507.

Wissler, M., Mazza, E., 2007. Electromechanical coupling in dielectric elastomer actuators. Sens. Actuators A Phys. 138 (2), 384–393.

Zhao, X., Hong, W., Suo, Z., 2007. Electromechanical hysteresis and coexistent states in dielectric elastomers. Phys. Rev. B 76, 134113.

Zhao, X., Suo, Z., 2008. Method to analyze programmable deformation of dielectric elastomer layers. Appl. Phys. Lett. 93, 251902.

Zhao, X., Suo, Z., 2010. Theory of dielectric elastomers capable of giant deformation of actuation. Phys. Rev. Lett. 104, 178302.